Analysis of Infrastructure to Support a Future Space Economy

Zayn A. Roohi*, Bradford Robertson†, and Dimitri N. Mavris‡
Georgia Institute of Technology, Atlanta, GA, 30332, USA

Beginning with the Artemis-I mission in late 2022, NASA is embarking upon a series of increasingly complex missions to establish a permanent presence on the surface of the Moon, potentially leading to manned Mars missions within the next few decades. Several private companies have also announced that they have begun work on space tourism projects with the goal of launching within this same time-frame. Supporting this expansion will require advanced space logistics and the development of dedicated space-based supply chains in order to reduce cost and increase resiliency. Previous research has focused on studying the impact that a specific technology, vehicle, or type of infrastructure has on supporting a single space campaign or mission; this paper takes a wider view by examining the impact that several types of infrastructure concepts together will have on the entire set of operations that could take place within the next decade. Lunar in-situ resource utilization, space depots, and space tugs are considered as infrastructure concepts, and a Lunar space station, Lunar habitat, Earth space stations, and Mars missions are considered as the operations to support. A time expanded mixed-integer nonlinear programming model is used to solve traditional network flow and supply chain problems, the results of which are used to propose future resupply missions and supply chain architectures.

I. Nomenclature

$\mathcal{A}$	=	All of the arcs within a network
C	=	Amount of supplies consumed by a specific demand or piece of infrastructure
$\mathscr{C}$	=	Cost of a particular item
DDTE	=	Design, Development, Testing, and Evaluation
$\mathcal{E}$	=	Maximum amount of propellant a specific vehicle can store and use
$\mathcal{F}$	=	Total flow of supplies along an arc. Flow of individual supply types are identified by subscript, such as $\mathcal{F}_{Water}$
$\mathscr{F}$	=	Objective function
g_0	=	Gravitational constant on Earth, 9.81 $\frac{m}{s^2}$
$\mathcal{I}$	=	Binary value representing whether a particular infrastructure concept exists in the solution or not
I_{sp}	=	S pecific impulse of a vehicle
$ISRU$	=	In-situ resource utilization
K	=	Percentage of a specific supply generated by ISRU and not converted into other supplies
LV	=	Launch vehicle
$\mathcal{M}$	=	Volumetric capacity of a vehicle
m_e	=	Empty mass of a vehicle
m_{H_2O}	=	Mass of water produced by Lunar ISRU
m_{LH_2}	=	Mass of liquid hydrogen produced by Lunar ISRU
m_{LO_x}	=	Mass of liquid oxygen produced by Lunar ISRU
m_{O_2}	=	Mass of breathable oxygen produced by Lunar ISRU
m_p	=	Payload mass being carried by a vehicle
m_{prop}	=	Mass of propellant produced by Lunar ISRU
m_t	=	Total mass of a vehicle, including its empty mass, propellant mass, and payload mass
MTV	=	Mars Transfer Vehicle

*Graduate Research Assistant, Aerospace Systems Design Laboratory, School of Aerospace Engineering.
†Research Engineer II, Aerospace Systems Design Laboratory, School of Aerospace Engineering, AIAA Member.
‡S. P. Langley NIA Distinguished Regents Professor, Boeing Regents Professor of Advanced Aerospace Systems Analysis, Director Aerospace Systems Design Laboratory, School of Aerospace Engineering, AIAA Fellow.

$\mathcal{N}$	=	Number of vehicles used
$\mathcal{O}$	=	Binary variable representing whether a node in space is a route origin for space tugs
$\mathcal{P}$	=	Propellant consumed by a vehicle while traveling along a specific arc
$\mathcal{Q}$	=	Payload or storage capacity of a specific vehicle or piece of infrastructure
$\mathcal{R}$	=	Quantity of supplies produced at a source
r_1	=	Radius of the originating orbit, measured from the center of the nearest body
r_2	=	Radius of the destination orbit, measured from the center of the nearest body
r_{b1}	=	Radius of the body that the originating orbit is around
r_{b2}	=	Distance from the center of the originating body to the center of the destination body
$\mathcal{T}$	=	Number of trips taken by a vehicle along a specific arc
$t_{delivery}$	=	The maximum time for a delivery window
t_{sim}	=	Time length of the model
TOF	=	Time of flight of a given arc or route
$\mathcal{V}$	=	Volumetric flow along an arc
$\mathcal{X}$	=	A binary variable representing whether a given route between two specified points is being used
Δv	=	Difference in velocity required to transfer between two orbits
μ	=	Standard gravitational parameter of a body
τ	=	A set representing all time steps

II. Introduction

In the coming decades, several of the major spacefaring nations have plans to begin a large-scale expansion into cislunar space. These plans range from private space stations for tourism to permanent manned habitats on the Moon and resupply and aggregation sites for manned missions to Mars. NASA in particular has plans with the European Space Agency, Canadian Space Agency, and others to return to the Moon, a program which began in late 2022 with the launch of Artemis-I [1]. Following this mission, they plan to assemble a space station in Lunar orbit, the Gateway, before establishing a permanent manned presence on the surface of the Moon itself. This expansion will be a radical departure from space operations of the present, where the only permanent manned operations are space stations in Low Earth Orbit. Such a change will require an equivalent change in the way in which operations are resupplied and supported. For example, the International Space Station (ISS) is currently resupplied directly from Earth every 2-3 months using launch vehicles, an approach that will become much more complex and expensive when supplying permanent operations further out into cislunar space.

Early space logistics studies in this area focused on only one specific aspect of this problem, studying vehicle routes [2], orbital traffic management [3], or resupply quantities and intervals [2]. Many of these studies were focused around the ISS, as it was the first permanent manned presence in space. A discrete event simulation tool named SpaceNet was developed and maintained by MIT between 2007-2012, and was used for a large number of studies during this time period [4]. However, inherent limitations of discrete event simulations meant that many aspects of the problem, such as vehicle routes and architecture optimization, could not be fully studied. A more recent approach has been to use mathematical models, such as Mixed-Integer Programming (MIP). These models have been used to solve traditional supply chain problems since the 1950s, and were first applied to space logistics as a part of a 2006 study presented at the SpaceOps Conference in Rome [5]. Their use has rapidly expanded over the past decade, with a majority of new space logistics studies utilizing either Mixed-Integer Liner Programming (MILP) or Mixed-Integer Non-Linear Programming (MINLP). These studies have utilized MIP models in order to solve mission architectures or optimize network flow between two points [6]. Several recent studies have taken the modeling effort a step further, introducing vehicle sizing and potential future technology. This has allowed for results to be produced on what technology or vehicle design an organization should invest in to support specific future space missions [7, 8]. Other research in the same vein has introduced infrastructure concepts such as propellant depots, and then has conducted trade studies on how these concepts effect supply flow and cost for a campaign [9–11].

The major contribution of this paper is to build upon previous research by modeling an entire future space economy within an integrated environment that considers multiple suppliers, missions, and supporting infrastructure types over a long range of time. This is done using methods developed for analogous Terrestrial supply chain problems, where the question being answered is what the topology of a network structure looks like to best minimize cost. Similar to these problems, this paper develops a solution by first designing a core graph network that contains route and cost information for a given case study. The Generalized Multi-Commodity Network Flow (GMCNF) and routing problems are then

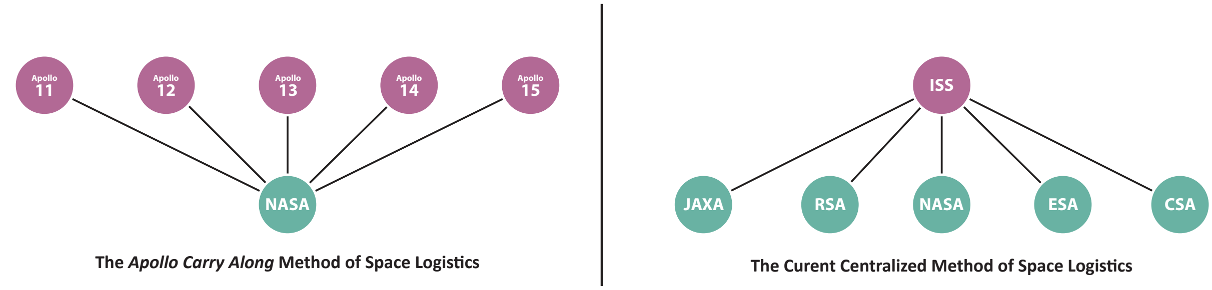

Fig. 1 Visualization showing the "carry-along" method used by NASA during the Apollo Missions (left), and the current method used to resupply the International Space Station (right) [6]

implemented using a Mixed-Integer Programming model that relies upon the graph network to determine route costs, transit lengths, and transit times. Given three feasible types of space infrastructure found via literature review, and a case study representing 2035, the model then determines the optimal solution for the objective of minimum cost.

III. Background

The practical side of space logistics stretches back to the early days of NASA and the Apollo missions. During this time period, planning was undertaken to support astronauts and operations on short trips the Moon. A method known as "carry-along" was employed [12], where each individual mission carried all of the supplies it needed for both supporting the astronauts and space vehicle in addition to those needed for emergencies. All of the supplies, mission planning, and logistics were produced on Earth and brought to the vehicle prior to launch, and post launch the only interactions between the mission and Earth were those via radio with Mission Control.

This approach is still used when it comes to unmanned research probes. Support operations for the ISS take a different approach. Resupply involves use of a centralized distribution network, where all supplies are produced and launched from Earth directly to the space station [12]. Logistics planning revolves around launch schedules, supply quantities, and traffic management. While this approach works well for the ISS, use of a centralized distribution network will be highly inefficient and may invite failures if it is used to support permanent operations deeper into space. This

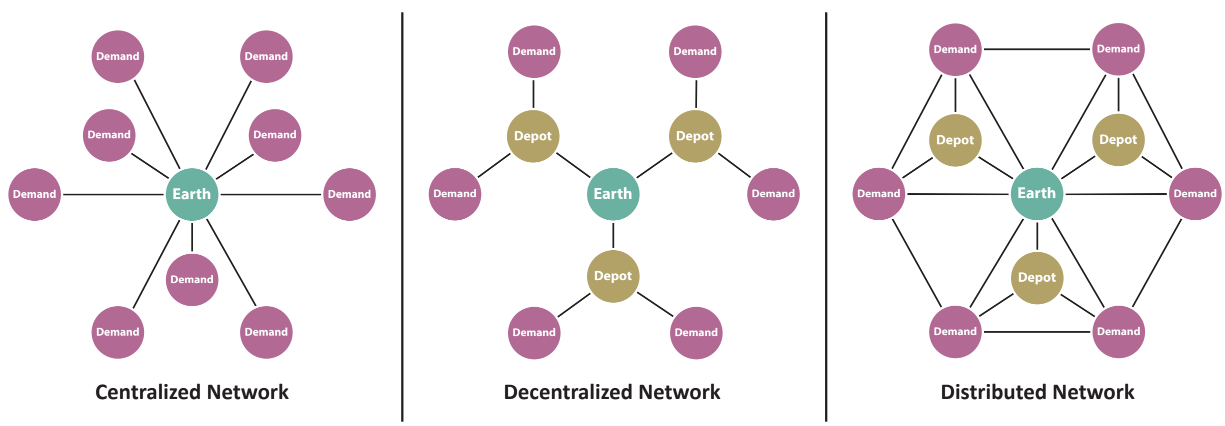

Fig. 2 Visualization of three different types of network structures that could be used to design future space logistics networks. Centralized networks (left) represent the way the International Space Station is resupplied in the present

method can be compared with an ideal future space logistics network, which could take the form of a decentralized or distributed network [12]. In such a network, supplies could be produced on both the Earth and the Moon, dedicated reusable space vehicles would be used for transit between orbits, and supply depots would be placed at key points for supply storage and distribution. Such a network has the potential to reduce propellant consumption and cost through use of reusable vehicles that are sized specifically for the routes they take. Use of depots would allow for supply storage in case of emergencies, and production of resources on the Moon would allow for supplies to be launched into orbit at a lower cost due to the low gravity of the Moon. In the distant future, supply production on Mars or asteroid mining could be a key part of reducing cost, and would further distribute the network load. Use of orbital manufacturing for parts or space craft could additionally reduce cost, particularly if Lunar regolith was used as the supply.

IV. Developing a Network Framework

Environment development begins with the creation of a graph network representing space, which can be used to determine the Δv needed for orbital transfers. On this graph network, every node represents a single orbit, and edges represent the possible paths between those orbits. The majority of commonly studied orbits within cislunar space are included in the network, as well as Martian orbits that are relevant to a future Mars campaign. On the graph network, all of the space nodes are connected to each other in order to maximize flexibility for path generation. However, Earth connects only to Low Earth Orbit (LEO), Mars only to Low Mars Orbit (LMO), and the Lunar South Pole only to Low Lunar Orbit (LLO).

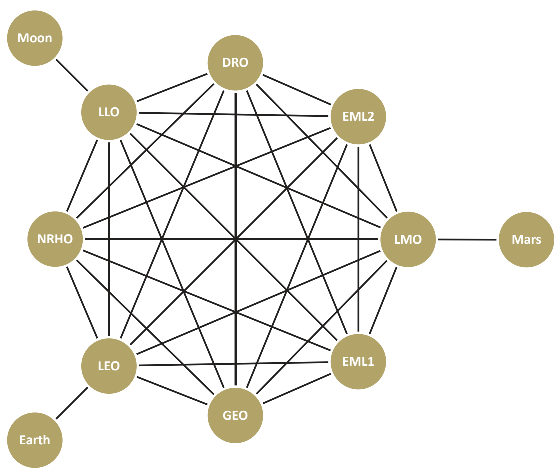

Fig. 3 Visualization of a subset of the graph network, showing the interconnectedness of different orbits

The edges of the graph network are double weighted with both the time of flight to travel along that edge and the Δv it takes to travel from one orbit to another. Both of these values are calculated using orbital mechanics simulations independent of the Mixed-Integer Programming model. Standard Hohmann Transfers are used for edges between orbits around the same body (i.e. LEO to GEO), and the Patched Conics method is used for edges between orbits around different bodies (i.e. GEO to LLO). Simplified versions of the equations used can be found as Equations 1 and 2.

$$\Delta v_{total} = \sqrt{\frac{\mu}{r_1}}\left(\sqrt{\frac{2r_2}{r_1+r_2}}-1\right)+\sqrt{\frac{\mu}{r_2}}\left(1-\sqrt{\frac{2r_1}{r_1+r_2}}\right) \tag{1}$$

$$\Delta v_{total} = \sqrt{\left(\sqrt{\frac{\mu_{b1}}{r_{b2}}}-\sqrt{\frac{2\mu_{b1}r_{b1}}{r_{b2}(r_{b1}+rb2)}}\right)^2+\frac{2\mu_{b2}}{r_2}}-\sqrt{\frac{\mu_{b2}}{r_2}} \tag{2}$$

These calculations are made under the assumption of perfectly circular orbits, and the radius used is the average value of the elliptical orbit. All angular calculations are ignored, it is assumed that there are no differences in the originating and ending angular arguments. For highly elliptical orbits such as NRHO, published data from NASA is used instead of any calculations, as the method using average radii is not accurate. Where available, the numbers calculated can be compared with official sources in order to verify their accuracy. Doing so shows that the Δv and time of flight for most edges differ by no more than 5%, validating the calculation method.

Origin	Destination	Δv	Time of Flight
KSC	LEO	9400 $\frac{m}{s}$	0.0069 $days$
LEO	GEO	3932 $\frac{m}{s}$	0.22 $days$
LEO	LLO	4092 $\frac{m}{s}$	4.6 $days$
GEO	LLO	2015 $\frac{m}{s}$	4.3 $days$
GEO	NRHO	1483 $\frac{m}{s}$	4.0 $days$
LLO	LSP	1900 $\frac{m}{s}$	0.0034 $days$

Table 1 Table showing a sample of the values calculated for Δv and time of flight for use in constructing a graph network

V. Formulation of the Mixed-Integer Programming Model

With the network framework developed, the Mixed-Integer Programming model can be created. This model is non-linear (MINLP), as many of the constraints require quadratic terms. The model is created by first introducing three novel concepts for future infrastructure. Next, relevant commodity types are introduced, as is the time-expanded nature of the model being developed. Finally, time-expanded model constraints and the objective function are formulated for all of the vehicles, sources, sinks, and infrastructure types.

A. Infrastructure Concepts

A large number of concepts for space-based infrastructure have been proposed over the past several decades. These concepts range from practical to infeasible given current technology, with various levels of research existing for each concept. This can be seen in concepts such as asteroid mining to support orbital spacecraft manufacturing, space farming, or building factories in orbit, all of which are unlikely to come to fruition within the next few decades. However, there are three key concepts that have been specifically mentioned by NASA or ESA as a part of either the Artemis program or manned Mars missions: space tugs, supply depots, and Lunar In-Situ Resource Utilization (ISRU).

The idea of using space tugs to reduce cost has existed since the end of the Apollo program [13]. Recent interest in their use has risen due to the Artemis missions, as research has shown that tugs can be used to resupply the Gateway from Earth Orbit, or for more localized transfer between orbits around the same body [14]. Tugs can potentially reduce cost both through their re-usability, and because they can increase the payload mass carried beyond Earth orbit as compared with current launch vehicles [14]. A recent design for a space tug is presented below in Table 2, and is used in the model developed.

Attribute	Value
Empty Mass	$2,165kg$
Payload Mass	$8,000kg$
Propellant Mass	$11,587kg$
I_{sp}	$445s$

Table 2 Basic attributes defining the space tug [15]

The concept of supply depots goes hand in hand with that of space tugs, and has existed almost as long [16]. Space depots provide an orbital location for supplies to be stored so that the space tug can access and deliver them when needed. Many proposed mission architectures rely upon depots with a large capacity that are resupplied with heavy launch vehicles, such as the Falcon Heavy, and a space tug then slowly distributes the supplies over the next several months [17].

Capacities generally range between 10,000 kg and 1,000,000 kg [18], depending upon the exact mission architectures modeled. Similar to space tugs, interest has risen in using depots since NASA announced the Artemis missions.

The final infrastructure concept that can be considered realistic for development within the next few decades is Lunar ISRU. Lunar ISRU relies upon ice mined from the Moon, and uses it to produce water, oxygen, or propellant [19]. Similar to concepts for depots, ISRU units have been studied at all sizes, from $1,000kg/yr$ test units to $1,000,000kg/yr$ industrial scale units [19]. Use of ISRU is mentioned several times in regards to building sustainable infrastructure during the Artemis missions [20], and a 2023 launch of a test drill for ISRU is planned as a collaboration between NASA and Intuitive Machines [21].

Launch Vehicle	Propellant	Payload Volume	LEO	GEO	TLI
Falcon 9 [22]	$488,370kg$	$145m^3$	$22,800kg$	$8,800kg$	-
Falcon Heavy [22]	$1,279,770kg$	$200m^3$	$63,800kg$	$26,700kg$	$17,200kg$
SLS Block 2 Cargo [23, 24]	$987,470kg$	$988m^3$	$150,000kg$	$75,000kg$	$46,000kg$

Table 3 Sample of the values used for three different launch vehicles in the MINLP model, including their propellant consumption, volumetric capacity, and the payloads to LEO, GEO and TLI

Two additional pieces of infrastructure are important to consider for any space logistics research and must be included in the model: launch vehicles and lunar landers. Unlike the three concepts discussed above, both of these types of infrastructure already exist or have been used in real world missions. Additionally, both of these types of infrastructure are a key part of the announced Artemis program, and money has already been spent developing them. Resupply missions generally use different launch vehicles at different times, and so it is important to include several alternatives in any space logistics studies. The attributes of three launch vehicles can be seen in Table 3. Information on a proposed reusable cargo lunar lander concept that uses LO_x and LH_2 as propellant can be found in Table 4.

Attribute	Value
Empty Mass	$3,500kg$
Payload Mass	$7,400kg$
Propellant Mass	$11,000kg$
I_{sp}	$450s$

Table 4 Basic attributes defining the lunar lander [25–27]

B. Commodities

In this formulation, only four commodities are considered: water, oxygen, food, and propellant. These four categories make up the majority of supplies delivered to the International Space Station [28], and future missions are likely to be the same. Estimates for these four commodities can be made using research on astronaut consumption and information about an mission's duration and population. These commodities are used, together with the graph network, to generate

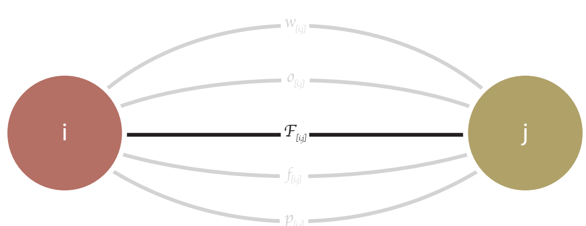

$$\mathcal{F}_{[i,j]} = \begin{bmatrix} Water_{[i,j]} \\ Oxygen_{[i,j]} \\ Food_{[i,j]} \\ Propellant_{[i,j]} \end{bmatrix} \quad (3)$$

Fig. 4 Visualization of the commodity flow between two nodes i and j (left) and the flow $\mathcal{F}_{[i,j]}$ for four commodities: water, oxygen, food, and propellant (right)

the set of all possible arcs, $\mathcal{A}$, between all nodes over the set of all times, τ. Flow between any two nodes i and j can then be said to be $\mathcal{F}_{[i,j]}$, a vector which is composed of the four commodity types. Commodity consumption and demand at a specific location and time can then be expressed as $\mathcal{F}_{[i,j]} = C_j$, assuming only node i brings supplies to j.

C. Time-Expanded Formulation

Mixed-Integer Programming models do not inherently account for time. The set of equations used to define the model are solved all at once, producing a solution that represents a single moment in time. The problem being solved in this paper requires time to be accounted for, as different operations are resupplied at different times, and these resupply missions need to be modeled as occurring at and over different times. This can be done by time-expanding the model, which requires the time dimension to be added to every equation and constraint. Instead of the set of arcs $\mathcal{A}$ representing a simple graph network where each node is a location and each arc is a possible path between those locations, the time-expanded network has added a new dimension to the problem, which means that travel can take place in both time and space [29, 30].

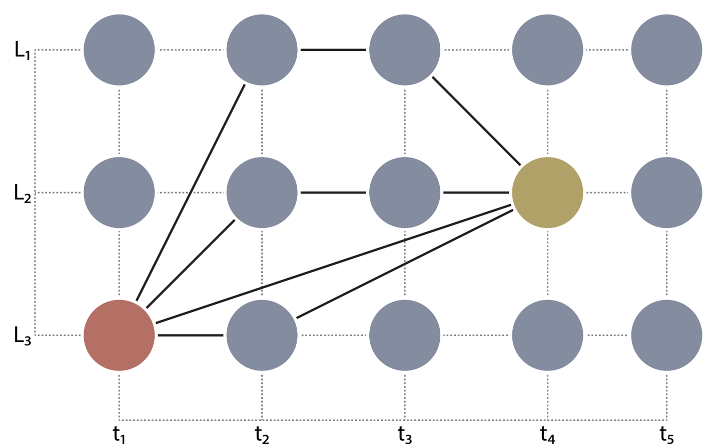

Fig. 5 Visualization of a simple time-expanded graph for three locations and five time steps, showing different routes through which a destination at (L_2, t_4) could be reached from an origin at (L_1, t_1)

A time step of 1-month is chosen for the model, which allows the problem to be constrained such that all missions and operations must have their cumulative supply requirements met by the end of each time step. This is done using a list of operations, their supply requirements, and their resupply intervals, which are all inputs to the model. This information is then used by the model to generate a list of demands at every one of the time steps, using the assumption

Time Step	Demand Name	Water	Oxygen	Food	Propellant
1	-	-	-	-	-
2	-	-	-	-	-
3	International Space Station	1,278 kg	319 kg	1,820 kg	907 kg
4	-	-	-	-	-
5	-	-	-	-	-
6	International Space Station	1,278 kg	319 kg	1,820 kg	907 kg
6	Gateway	1,825 kg	334 kg	2,600 kg	250 kg
6	Lunar Habitat	1,825 kg	334 kg	2,600 kg	50 kg

Table 5 Table showing several demands expanded over time

that all operations have 100% of their supplies at time step zero. At time step 1, all operations with a one-month resupply interval will need to be resupplied with $\frac{1}{12}$ of their yearly demands. At time step 2 all 2-month resupply intervals will need $\frac{1}{6}$ of their yearly demands, and so on. Table 5 shows a sample of time-expanded demands output by this process.

D. Model Formulation

The first constraint added to the model represents the commodity demands needed at each node in the network, also known as sinks, and can be seen in Equation 4. This equations states that the commodity inflow to any node must equal the commodity consumption at that node plus the commodity outflow from it. In this equation and all after, it is assumed that the propellant a spacecraft needs to travel along all arcs departing from a specific node is extracted from that specific node by the spacecraft prior to its departure. Manned Mars missions represent a special type of sink in the model. A specified demand is assumed to be needed on the surface of Mars to support the mission, and the model additionally includes all of the supplies consumed while traveling to Mars and back. While the presence and population of the Mars mission is an input, the route of the Mars transfer vehicle and the location where it is supplied in cislunar space are optimized for with the infrastructure, so that the Mars mission architecture itself is integrated with the infrastructure solution. The model is set up such that this vehicle can be aggregated and transfer to Mars from any non-Earth orbit, as many proposals for a Mars transfer vehicle set this requirement. This means that in addition to Equation 4, an additional set of constraints representing the Mars transfer vehicle's supply consumption and payload capacity are needed. These can be found as Equations 5 and 6.

$$\sum_{[i,D]\in\mathcal{A}} \mathcal{F}_{[i,D,t]} = C_{[D,t]} + \sum_{[D,j]\in\mathcal{A}} \left(\mathcal{F}_{[D,j,t]} + \mathcal{P}_{lander_{[D,j,t]}} + \mathcal{P}_{tug[D,j,t]}\right) \quad \{\forall D \in Demands \ \wedge \ \forall t \in \tau\} \tag{4}$$

$$\mathcal{F}_{[i,Mars,t]} = C_{[i,Mars,t]} + \mathcal{P}_{MTV_{[i,Mars,t]}} + C_{[Mars,t]} \quad \{\forall t \in \tau\} \tag{5}$$

$$\mathcal{F}_{[i,Mars,t]} \leq Q_{MTV} \quad \{\forall t \in \tau\} \tag{6}$$

In Equations 4 and 5, the amount of propellant $\mathcal{P}_{i,j,t}$ is calculated using the Tsiolkovsky rocket equation, given the Δv value for a specific arc $\mathcal{A}_{[i,j]}$ and information about the vehicle traveling along it. The basic rocket equation takes the form of $\Delta v = I_{sp} g_0 \ln \frac{m_t}{m_e}$, and can be rewritten in the form seen as Equation 7 for the purposes of solving for propellant consumption along an arc. For this use, Equation 7 is an accurate method of estimating propellant consumption, with any error originating from the underlying assumptions about the vehicle itself, or from the prior calculation of Δv in the graph network.

$$\mathcal{P}_{vehicle_{[i,j,t]}} = (m_e + m_p) e^{\frac{\Delta v_{[i,j]}}{I_{SP} * g_0}} - m_e \tag{7}$$

The two sources, Earth and Lunar ISRU, are represented primarily through a simple constraint that requires the flow output from each location to be lower than the amount of supplies produced between time zero and the current time t_c. As the Earth is assumed to have no production-rate limits, this constraint only practically applies to Lunar ISRU. It can be seen as Equation 8, which also includes a term to account for the propellant consumed by lunar landers on the Moon and launch vehicles on Earth. A second constraint prevents supplies from flowing back into a source, which can be seen as Equation 9. An additional set of constraints for the ISRU unit are added to the model to allow for the production rate and size of the ISRU unit to be optimized for. The constraints written represent the physical chemical reactions that govern the conversion of H_2O into H_2, O_2, LO_x, and LH_2, and they can be seen as Equations 10, 11, 12, 13, and 14 (Equation 15 represents the mixing constraint when creating propellant). The factor K is introduced to represent how much of a particular supply is kept in its original state, and how much is used to create other supplies. These K-factors are optimized as a part of the model. As written below, these constraints are in their mass balance form and not the molar-mass form more generally seen with chemical equations, as that is the way they are built into the model. One key assumption made in regards to ISRU is that all vehicles using the propellant produced will be propelled by liquid oxygen (LO_x) as the oxidizer and liquid hydrogen (LH_2) as the fuel. The tug and lunar lander concepts integrated into the model both meet this requirement.

$$\sum_{t=0}^{t_c} \sum_{[S,i]\in\mathcal{A}} \left(\mathcal{F}_{[S,i,t]} + \mathcal{P}_{lander_{[S,i,t]}} + \mathcal{P}_{LV_{[S,i,t]}}\right) \leq \sum_{t=0}^{t_c} \mathcal{R}_{[S,t]} \quad \{\forall S \in Sources \ \wedge \ \forall t_c \in \tau\} \tag{8}$$

$$\sum_{[i,S]\in\mathcal{A}} \mathcal{F}_{[i,S,t]} = 0 \quad \{\forall S \in Sources \ \wedge \ \forall t \in \tau\} \tag{9}$$

$$m_{H_2O} = K_{H_2O}\mathcal{R}_{ISRU} \tag{10}$$

$$m_{O_2} = 0.89K_{O_2}\mathcal{R}_{ISRU}(1 - K_{H_2O}) \tag{11}$$

$$m_{LH_2} = 0.11\mathcal{R}_{ISRU}(1 - K_{H_2O}) \tag{12}$$

$$m_{LO_x} = 0.89\mathcal{R}_{ISRU}(1 - K_{H_2O})(1 - K_{O_2}) \tag{13}$$

$$m_{prop} = LO_x + 6LH_2 \tag{14}$$

$$K_{O_2} \leq 0.26 \tag{15}$$

Depots are modeled as points through which supplies can flow if space vehicles or lunar landers are being used. They are not required to exist in the model, as launch vehicles can deliver supplies directly to any given demand instead, if that solution is more optimal. Depots can exist at any point in space, and the main constraints governing their use are for flow continuity, Equation 16, and their capacity, Equation 17. The time expansion of depots allows for supplies to be stored for up to six months so that excess supplies produced or launched in an earlier time step can be used in a future time step. Each individual depot can have a different capacity, the exact value of which is optimized for.

$$\sum_{t-6}^{t}\sum_{[i,D]\in\mathcal{A}} \mathcal{F}_{[i,D,t]} \geq \sum_{t-6}^{t}\sum_{[D,j]\in\mathcal{A}} \left(\mathcal{F}_{[D,j,t]} + \mathcal{P}_{tug_{[D,j,t]}} + \mathcal{P}_{lander_{[D,j,t]}}\right) \quad \{\forall D \in Depots \ \wedge \ \forall t \in \tau\} \tag{16}$$

$$\sum_{t-6}^{t}\sum_{[i,D]\in\mathcal{A}} \mathcal{F}_{[i,D,t]} - \sum_{t-6}^{t-1}\sum_{[D,j]\in\mathcal{A}} \left(\mathcal{F}_{[D,j,t]} + \mathcal{P}_{tug_{[D,j,t]}} + \mathcal{P}_{lander_{[D,j,t]}}\right) \leq Q_D \quad \{\forall D \in Depots \ \wedge \ \forall t \in \tau\} \tag{17}$$

There are four different types of constraints which can be applied to vehicles in this formulation: vehicle mass capacity, vehicle volumetric capacity, vehicle propellant capacity, and vehicle propellant consumption. Launch vehicles originate from Earth and travel to specific destinations, so launch vehicle propellant is assumed to have been extracted from Earth and is not be accounted for further in this model. Data on the payload capacity to various orbits is readily available for existing launch vehicles and can be used to construct the mass and volumetric flow constraints. These constraints can be seen in Equations 18 and 19. As this dataset implicitly accounts for propellant capacity of the launch vehicle, no additional constraints are added.

$$\mathcal{F}_{[Earth,i,t]} \leq Q_{LV}\mathcal{N}_{LV_{[i,t]}} \quad \{[Earth,i] \in \mathcal{A} \ \wedge \ \forall t \in \tau\} \tag{18}$$

$$\mathcal{V}_{[Earth,i,t]} \leq \mathcal{M}_{LV}\mathcal{N}_{LV_{[i,t]}} \quad \{[Earth,i] \in \mathcal{A} \ \wedge \ \forall t \in \tau\} \tag{19}$$

Space tugs and lunar landers are implemented in the model similarly to launch vehicles, but additionally include constraints related to vehicle propellant capacity and vehicle propellant consumption. Volumetric constraints are not included for these vehicles, as it is not available in the existing literature that the concepts were sourced from. Propellant consumption is accounted for in the prior source, sink, and depot equations presented. As the model assumes that propellant is extracted from each node prior a vehicle traveling along its next arc, it needs to account for the ability of vehicles to bring extra propellant in their propellant tank for traveling along other arcs in a specific route. This propellant constraint is coupled with the capacity constraint, and both can be seen as Equations 20 and 21 respectively. A final vehicle constraint is required to ensure that arcs are not longer than vehicles have the propellant for, which can be seen in Equation 22.

$$\mathcal{F}_{[i,j,t]} + \mathcal{P}_{vehicle[i,j,t]} \leq (Q_{vehicle} + \mathcal{E}_{vehicle}) * \mathcal{T}_{vehicle[i,j,t]} \quad \{\forall [i,j] \in \mathcal{A} \ \wedge \ \forall t \in \tau\} \tag{20}$$

$$\mathcal{F}_{Water_{[i,j,t]}} + \mathcal{F}_{Oxygen_{[i,j,t]}} + \mathcal{F}_{Food[i,j,t]} \leq Q_{vehicle} \mathcal{T}_{vehicle[i,j,t]} \quad \{\forall [i,j] \in \mathcal{A} \ \wedge \ \forall t \in \tau\} \tag{21}$$

$$\mathcal{P}_{vehicle[i,j,t]} \leq \mathcal{E}_{vehicle} \quad \{\forall [i,j] \in \mathcal{A} \ \wedge \ \forall t \in \tau\} \tag{22}$$

The final set of constraints added are those related to vehicle routing. While the previously presented flow constraints look at the direct supply flow between two nodes, routing constraints look at the overall route taken between a source and a sink, which does not necessarily have to be direct. This allows for three major aspects of the problem to be solved: how many vehicles are needed, where they are needed, and what routes they should take. An initial routing constraint is introduced such that routing paths are directly tied into the supply flow constraints introduced in the previous sections. The binary variable $\mathcal{X}_{[i,j,t]}$ can be introduced, representing whether a specific arc is used or not, and a constraint can be developed that requires all arcs with supplies flowing along them to be part of the final route. This is seen in Equation 23. As $\mathcal{X}_{[i,j,t]}$ is a binary variable, this equation includes an arbitrarily large number to ensure that the inequality can be met when $\mathcal{F}_{[i,j,t]} > 1$. An important part of this constraint is that it allows an arc with zero supply flow to be part of a route, as empty vehicles need return to their origin point. Tying routes to supply flow in this way ensures that all subtours are eliminated, and vehicles will start and finish their routes at the required locations. The constraints requiring vehicles to return to their origin point can be seen in Equations 24 and 25.

$$\mathcal{F}_{[i,j,t]} \leq 10^8 \mathcal{X}_{[i,j,t]} \quad \{\forall [i,j] \in \mathcal{A} \ \wedge \ \forall t \in \tau\} \tag{23}$$

$$\sum_{[i,N] \in \mathcal{A}} \mathcal{X}_{[i,N,t]} = \sum_{[N,j] \in \mathcal{A}} \mathcal{X}_{[N,j,t]} \quad \{\forall N \in Nodes \ \wedge \ \forall t \in \tau\} \tag{24}$$

$$\sum_{[i,N] \in \mathcal{A}} \mathcal{T}_{vehicle[i,N,t]} = \sum_{[N,j] \in \mathcal{A}} \mathcal{T}_{vehicle[N,j,t]} \quad \{\forall N \in Nodes \ \wedge \ \forall t \in \tau\} \tag{25}$$

Extraneous paths can be eliminated by implementing a delivery window, which allows for the optimization and solution finding process to be sped up. This can be seen in Equation 26. While 30 days is the logical option here given the one-month time step, a a delivery window representing the minimum resupply interval is used instead. For example, a network consisting of operations that are resupplied at minimum every three months will result in the model using a 90-day delivery window. This is a more realistic delivery window as a vehicle can practically begin its resupply route for a set of operations the moment its mission has ended during the previous resupply window. Using this longer delivery window also allows for depots to be located further away from demands, such as placing them at the Lagrange 4 and 5 points. Fewer tugs can be used, as resupplying large demands like the Mars transfer vehicle can be stretched out over a longer time period. A similar constraint can be added for the entire set of routes, requiring that all operations are resupplied within this delivery window (Equations 27 and 28).

$$\mathcal{X}_{[i,j,t]} TOF_{[i,j]} \leq t_{delivery} \quad \{\forall [i,j] \in \mathcal{A} \ \wedge \ \forall t \in \tau\} \tag{26}$$

$$\sum_{[i,j] \in \mathcal{A}_{Tugs}} \left(\mathcal{X}_{[i,j,t]} TOF_{[i,j]} \right) \leq t_{delivery} * N_{Tugs} \quad \{\forall t \in \tau\} \tag{27}$$

$$\sum_{[i,j] \in \mathcal{A}_{Landers}} \left(\mathcal{X}_{[i,j,t]} TOF_{[i,j]} \right) \leq t_{delivery} * N_{Landers} \quad \{\forall t \in \tau\} \tag{28}$$

The final part of the routing problem is to determine where vehicles are placed, which in turn determines where routes begin and end. To minimize assumptions, it is not required that every depot has an attached space tug, or that only depots can be route origins. Instead, the routing constraints are set up such that any node in space can be a tug route origin, and depots can exist without attached tugs. Two requirements are set for a node to be a tug route origin: more supplies must be flowing in from Earth than are consumed at that node, and supplies must be flowing out of that node. This can be seen in Equation 29, where O is a binary variable representing whether the node is a tug route origin. As O is a binary variable, similar to Equation 23, an arbitrarily large number is required to ensure the inequality is met when

$\mathcal{F}_{[i,j,t]} > 1$. The number of tugs must be greater than or equal to the number of tug origin nodes, as seen in Equation 30. It is assumed the the route origin for all lunar landers is the Lunar South Pole, where a Lunar habitat is located.

$$\left(\mathcal{F}_{[Earth,N,t]} - C_N\right) \sum_{[N,i]\in\mathcal{A}} \mathcal{F}_{[N,i,t]} \leq 10^8 O_N \quad \{\forall N \in Nodes \ \wedge \ \forall t \in \tau\} \tag{29}$$

$$\sum_{N\in Nodes} O_N \leq N_{Tugs} \tag{30}$$

E. Objective Function

The objective is to minimize the cost of resupplying all operations in the network. The objective function developed represents the tradeoff between resupplying all operations directly from Earth, as space logistics are done now, and investing in the three novel infrastructure concepts presented in section V.A, which can potentially reduce cost. This is done through three broad terms, as seen in Equation 31: the total design, development, test and evaluation (DDTE) cost, the infrastructure launch cost, and the operational supply cost of the network. The first two terms in this equation represent the infrastructure, and the third represents the cost to launch supplies on launch vehicles from Earth.

$$\mathscr{F} = \mathscr{C}_{DDTE} + \mathscr{C}_{Launch} + \mathscr{C}_{Supplies} \tag{31}$$

DDTE costs, $\mathscr{C}_{DDTE}$, are obtained through standard NASA cost estimation techniques, including the NASA-Air Force Cost Model (NAFCOM), Spacecraft Vehicle Level Cost Model (SVLCM), and the Advanced Missions Cost Model (AMCM) [31], and depend on whether a specific infrastructure concept is present in a given solution or not.

$$\mathscr{C}_{DDTE} = \mathscr{C}_{DDTE_{Depot}} \mathcal{I}_{Depot} + \mathscr{C}_{DDTE_{Tug}} \mathcal{I}_{Tug} + \mathscr{C}_{DDTE_{ISRU}} \mathcal{I}_{ISRU} \tag{32}$$

The launch cost is determined using infrastructure mass and launch cost per unit mass to a specific orbit. Launch cost per unit mass in this equation comes from existing launch vehicle data, and the infrastructure mass is determined from models found during literature review. For ISRU, a linear model relating mass and yearly production rate presented in a recent NASA study is used [19]. A similar model is used for depot mass estimation. Literature review shows most depot concepts have a payload mass fraction between 70-90% [32]. The average of 80% is used, which means that depots have roughly four times as much payload capacity as they weigh: $m_{Depot} = 0.25 Q_{Depot}$. The empty mass of the space tug seen in Table 2 is used to determine its launch cost, as is the empty mass for the lunar lander shown in Table 4.

$$\mathscr{C}_{Launch} = \sum_{d\in depots} \mathscr{C}_{kg} m_d + \mathscr{C}_{kg} m_{tugs} N_{tugs} + \mathscr{C}_{kg} m_{ISRU} \tag{33}$$

The supply cost comes from the cost to launch supplies from Earth to a specified mission. If there is no infrastructure, then all supplies will launch from Earth, and this cost term will be higher. If infrastructure exists, ideally it will reduce the amount of supplies launched, lowering this cost while raising the costs in the other objective function equations shown. The objective function will the determine the optimal balance between these terms by finding the optimal location and capacities for different pieces of infrastructure.

$$\mathscr{C}_{Supplies} = \sum_{t=1}^{t_{sim}} \sum_{[i,j]\in\mathcal{A}} \mathscr{C}_{LV} N_{LV_{[i,j,t]}} \tag{34}$$

VI. Case Study: A 2035 Space Economy

A case study can be used to demonstrate the methodology and model developed in the previous sections. This case study is scoped to represent a future space economy composed of missions existing within the time-frame 2035 - 2055. All of the projects announced by NASA as a part of the Artemis program are included in this case study: a Lunar Habitat on the south pole of the Moon and the Gateway space station in a Near-Rectilinear Halo Orbit (NRHO). It is assumed that while the International Space Station has been retired, a replacement space station in LEO exists. Additionally, a private space station, such as Blue Origin's Orbital Reef, is assumed to exist in LEO. Manned Mars missions occur every five years, travelling between cislunar space and Mars via a reusable Mars Interplanetary Transfer Vehicle [33]. Finally, a form of satellite servicing is included, with propellant being consumed in both LEO and GEO by vehicles servicing a small subset of satellites every year.

Mission	Location
Lunar Habitat	Lunar South Pole
Gateway Space Station	NRHO
ISS Replacement	LEO
Private Space Station	LEO
Mars Missions	Mars
Satellite Servicer	LEO
Satellite Servicer	GEO

Table 6 Table of the different operations and missions that are included as a part of the case study

A. Operational Requirements

For this case study, all four types of supplies mentioned previously are considered in the multi-commodity flow problem: water, oxygen, propellant, and food. Requirements for the human consumables (water, oxygen, and food) are estimated using existing data from the International Space Station. This data can be seen in Table 7. Water re-use of 9 $kg/person/day$ [34] and oxygen generation of 2.34 kg/day [35] are additionally included in the case study.

Supply Type	Per Day	Per Year
Water	$11kg$	$4,015kg$
Oxygen	$0.834kg$	$304kg$
Food	$2.85kg$	$1,040kg$
Propellant	$9.9kg$	$3,629kg$

Table 7 Supplies required to sustain one human on the International Space Station for both one day and one year [34–36], not including supply re-use

Requirements for propellant for the case study are found through studying existing literature on orbit-keeping maneuver consumption. The two space stations in LEO use the value for the International Space Station displayed in Table 7 [36], and the value for the Gateway space station is based off of previous research [37]. Propellant consumption for the Mars Mission is calculated from the exact route the vehicle takes to get to Mars and back using data on a theoretical vehicle design published by NASA researchers [33]. The Lunar habitat is assumed to use a small amount of propellant every year for either exploration missions or as a safety margin for emergencies.

The two satellite servicers consume only propellant. As it is difficult to quantify the potential needs or market of any future satellite servicers, a conservative guess is used, assuming that they together resupply 1% of the existing satellites every year. Noting that the average satellite consumes $50kg$ of propellant per year [38], and that 55% of satellites are in LEO and 35% in GEO [39], propellant needs can be generated for the estimated 30,000 satellites that exist in 2035 [40].

Mission	Population	Water	Oxygen	Food	Propellant
Lunar Habitat	5	3,650 kg	668 kg	5,200 kg	100 kg
Gateway Space Station	5	3,650 kg	668 kg	5,200 kg	500 kg
ISS Replacement	7	5,110 kg	1,277 kg	7,280 kg	3,629 kg
Private Space Station	3	2,190 kg	547 kg	3,120 kg	3,629 kg
Mars Missions	4	2,920 kg	364 kg	4,161 kg	Varies
LEO Satellite Servicer	-	-	-	-	8,250 kg
GEO Satellite Servicer	-	-	-	-	5,250 kg

Table 8 Table of supply requirements for the case study

B. Resupply Intervals

Resupply intervals are input to the model that dictate the maximum time period between supply deliveries. In Earth orbit, manned operations are assumed to have resupply intervals of 3 months, and unmanned operations are assumed to have resupply intervals of 12 months. All manned operations not in Earth Orbit are assumed to have resupply intervals of 6 months. One key exception to these rules are the Mars Missions, which are not resupplied in a continuous fashion. These missions last three years [41], and therefore three years of supplies are needed every time one of these missions occurs, which is set to be every five years.

Operation	Resupply Interval
Earth-Orbit Manned Operations	3 months
Earth-Orbit Unmanned Operations	12 months
Lunar Operations	6 months
Mars Mission	60 months

Table 9 Table showing the resupply intervals used in the model

VII. Results

The case study is run several times as a part of different trade studies. A baseline study is first run with all infrastructure disabled, representing the current method of space logistics. Only launch vehicles existing today and lunar landers are present in this model. This baseline is used as a comparison point for different metrics, such as overall cost, number of launches, and network design. The second study includes the full set of infrastructure, and the reduction in overall cost and number of launch it creates are examined. Following this, a series of sensitivity studies are run where the types of infrastructure present in the simulation are varied in order to determine the type that impacts cost and launch metrics the most.

A. Baseline

As expected, the baseline case produces a network where supplies flow directly from Earth to their destination. The only exceptions to this are the Mars transfer vehicle, which carries supplies to Mars, and the Gateway, which sends supplies to the Lunar Habitat through a lunar lander. This behavior is expected, as it is the current plan for space logistics. The network flow and routing diagrams for the baseline solution can be seen in Figure 6. Multiple launches to the same destination are spaced out such that only one launch can occur per day, while launches to different destinations can happen on the same day, under the assumption that multiple launch pads are available.

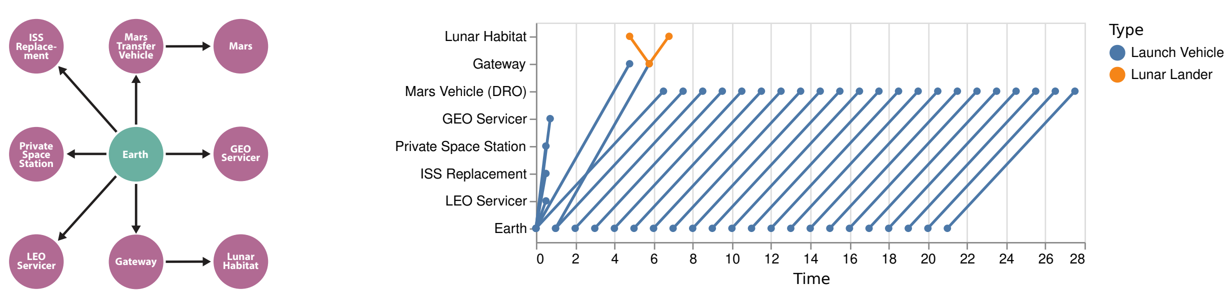

Fig. 6 Visualization of the network and supply flow solution for the baseline case with no infrastructure (left) and the routing solution (right)

B. Full Study

Running the model with infrastructure enabled produces results that are significantly different than the baseline. Table 10 shows the infrastructure results and key metrics for this case, and compares them with the baseline. Figure 7

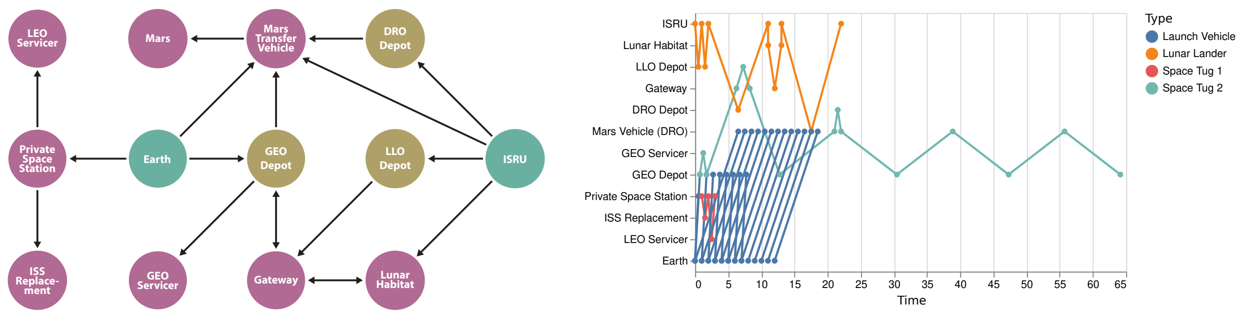

Fig. 7 Visualization of the solution for the full study, showing the network flow (left) and vehicle routing (right)

shows a visualization of the routing and network supply flow problems. These results show several key details. As seen in in Table 10, an integrated space logistics environment that examines both what infrastructure should be present and how vehicles and supplies flow allows for cost to be significantly reduced. This cost can be seen as directly tied to the number of launch vehicles needed. Launch vehicles can bring much larger payloads to LEO and GEO as compared with Lunar orbits, which means that the use of tugs and depots significantly reduces the number of launches needed, even though the total mass of supplies launched from Earth decreases by only 17%. Additionally, producing supplies on the Moon with an ISRU unit allows for the majority of the oxygen and water needed to be produced in that location, further lowering cost. Finally, strategically solving routes allows for the number of vehicles to be minimized, and for vehicles to carry supplies in both directions. This can be seen with the GEO depot tug, which primarily carries food from Earth to the Lunar orbits, and then carries propellant that originated at the ISRU unit back to the GEO Depot. The aggregation and resupply location of the Mars transfer vehicle is unchanged between the baseline and full study, in both a Distant Retrograde Orbit (DRO) is the optimal location.

Attribute	Baseline	Full Study	Difference
Cost	\$68,840,000,000	\$30,537,670,058	-55%
Earth Launches	368	180	-51%
Earth Launch Mass	2,364,044 kg	1,961,184 kg	-17%
Tug Trips	-	468	-
Lander Trips	40	152	280%
Depot Locations	-	GEO (80,000 kg) LLO (32,000 kg) DRO (31,000 kg)	-
ISRU Size	-	99,182 kg/yr	-
Tug Locations	-	Low Earth Orbit GEO Depot	-
Mars Vehicle Location	DRO	DRO	-

Table 10 Table containing the results for the baseline case and full study run, including the cost, launches, and infrastructure details

The flow network shown can be further broken down into its four individual supply components: water, oxygen, propellant, and food. Visualizing these breakdowns produces interesting results, as seen in Figure 8. From this diagram it can be seen that the ISRU unit produces all of the water and oxygen needed for the demands not in Earth orbit. All of the food is produced on Earth and flows out to the demands, as it cannot be produced anywhere else, and propellant is produced in both locations and distributed equally. As a part of the route optimization, it can be seen that the tug carries food from Earth to the LLO depot and then carries propellant and water back on its return journey. The extensive distribution of supplies, particularly propellant, illustrates exactly how use of an integrated space logistics environment

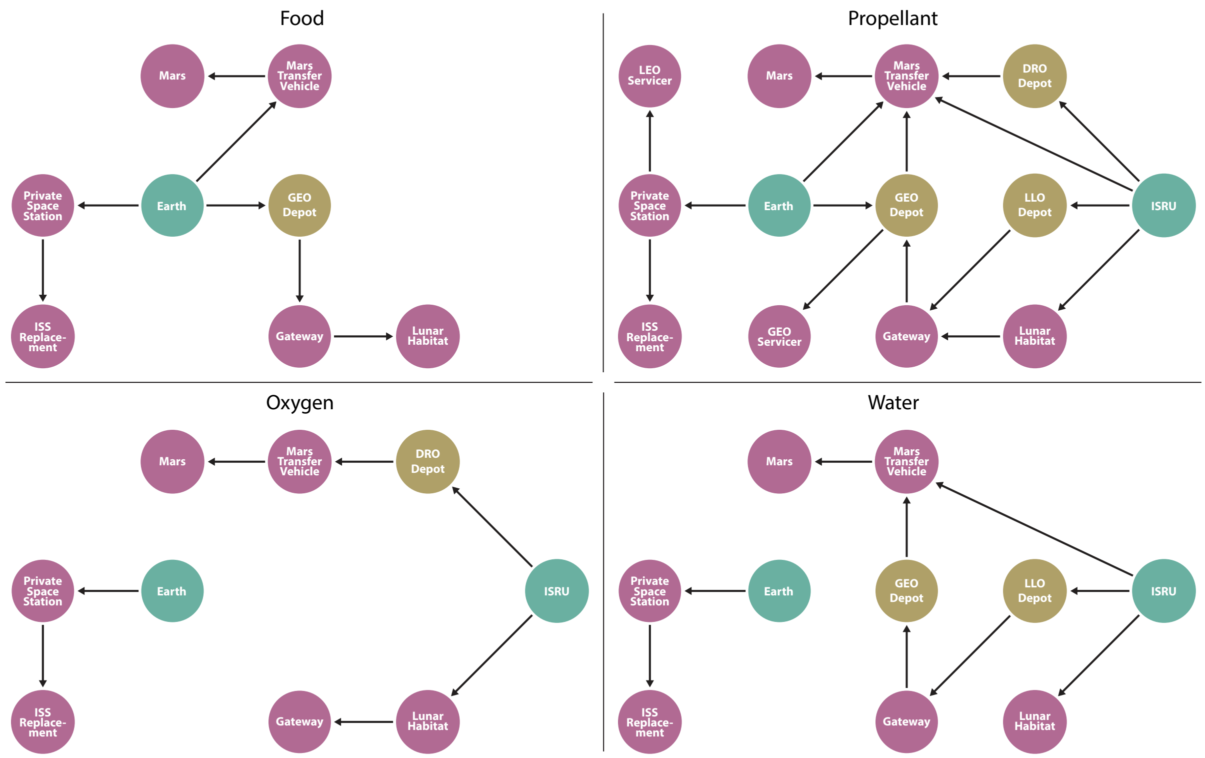

Fig. 8 Visualization of flow for the four different supply types: food (top left), propellant (top right), oxygen (bottom left), and water (bottom right)

can reduce cost. Without this type of planning, launch vehicles will be required to make all of the trips individually, with each launch potentially requiring an expendable vehicle. Use of a space tug and depots reduces the number of vehicles in use, and ISRU allows for supplies to be produced and launched more cheaply than on Earth. Additionally, when supplies are cheaper to produce and deliver from Earth, such as water and oxygen for space stations in Earth orbit, this integrated method of space logistics is able to find those solutions.

C. Infrastructure Sensitivity

This next study examines the sensitivity of the solution discussed previously to different types of infrastructure. The goal of this study is to determine what infrastructure or infrastructure combinations are the most effective at reducing cost, which in turn can guide recommendations on what should be given priority for development. This is done by

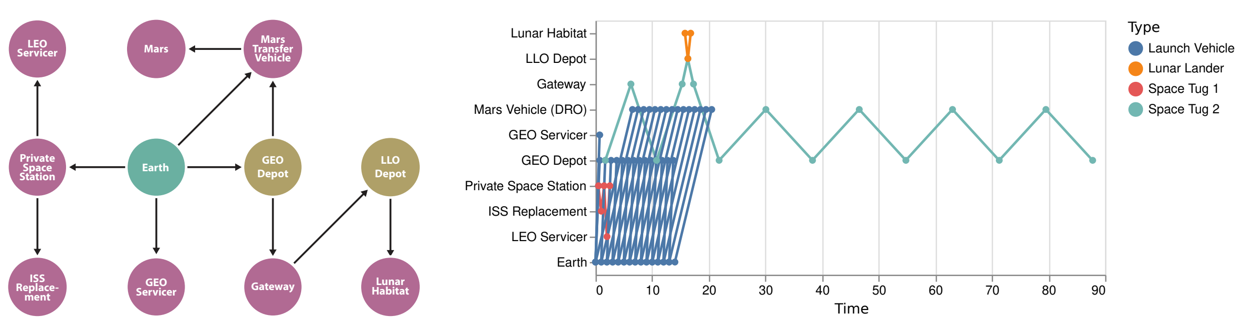

Fig. 9 Visualization of the solution of the infrastructure sensitivity study with only tugs and depots, showing the network flow (left) and vehicle routing (right)

first running the model with only one type of infrastructure allowed, and then re-running with most of the possible combinations of two types of infrastructure. The results of this study can be seen in Figure 10, which also includes the results from the baseline and full study for reference. A key omission in this sensitivity study is the impact of depots alone. It is not possible to study this, as the model developed mostly requires tugs to be present in order for depots to be used. Without tugs, depots can store and receive supplies from Earth, but cannot deliver them to any location other than the Lunar surface through a lunar lander.

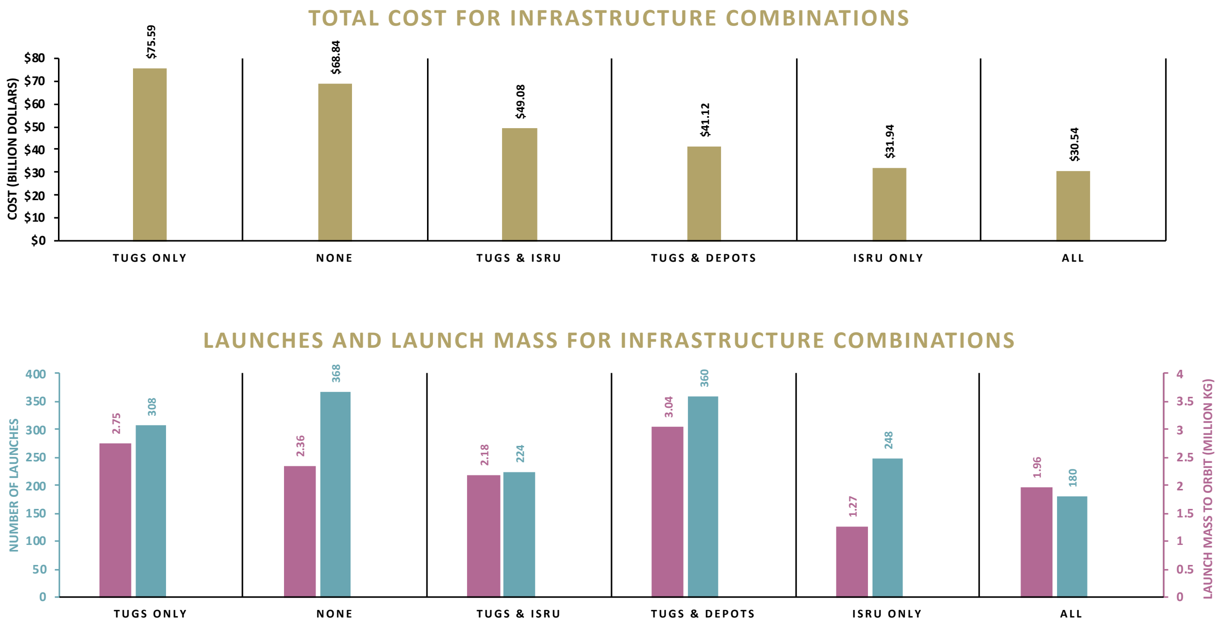

Fig. 10 Results from the infrastructure sensitivity study, showing the cost of different infrastructure combinations (top) and the launch vehicles and Earth launch mass required for the same combinations (bottom)

The infrastructure most effective at reducing cost is clear: Lunar ISRU. ISRU alone is able to reduce cost by 53%, as compared with a 55% reduction when all three types of infrastructure were present. The cost saving presented by the ISRU is due to multiple reasons. First, supplies can be launched off of the Moon much more efficiently than Earth due to the lower gravity. Proposed cargo lunar lander concepts are generally 60% propellant and 25% payload [42], versus launch vehicles, which are around 90% propellant and less than 3% payload [43]. Additionally, the Mars transfer vehicle is aggregated and resupplied in a Distant Retrograde Orbit, which means that the resupply arc from the Lunar South Pole has a lower Δv cost than an arc from Earth. Finally, as the lunar lander must routinely travel to the Gateway and LLO Depot in order to bring food down to the Lunar Habitat, carrying water and oxygen on the initial trip to the Gateway does not require extra travel. The results of this study also show that tugs are not a cost-effective investment when used alone. Tugs alone increased cost by 10% and required 17% more supply mass to be launched from Earth. This result is likely because alone, tugs can only carry supplies from one location to the next, and each individual location cannot store a large amount of extra supplies if supply depots are not present. This point is proven by the results for tugs and depots, which together are able to reduce cost by 40% as compared with the baseline.

VIII. Conclusion

This paper proposes a method for developing an integrated environment that simulates a future space economy and the infrastructure needed to support it. In this environment, the missions simulated as a part of the economy are fixed inputs, while supporting infrastructure is optimized in order to lower overall cost over a given time period. A model for evaluating costs is used that considers initial DDTE costs and operational costs.

A case study representing the future Artemis missions, a private space station, and manned Mars missions is used to demonstrate the abilities of the model. Analysis of the results shows that use of infrastructure and logistics planning can reduce overall mission cost by 55% as compared with a baseline where all missions are resupplied using current methods with no infrastructure or logistics. Further studies examine the impact that different arrangements of infrastructure have on cost in order to provide a recommendation on which are the most useful. The results of this series of studies show that Lunar ISRU alone can reduce cost by 53% and in-orbit supply depots and tugs together by 40%. These findings lead to the recommendation that further research and development into ISRU, space tugs, and in-orbit supply depots is undertaken, as their cost reduction potential is large. The findings also show that all three types of infrastructure are not required to reduce cost, so development activities are not constrained to bring all three technologies to fruition at once.

References

[1] "The Artemis Plan: NASA's Lunar Exploration Program Overview," Tech. rep., National Aeronautics and Space Administration, September 2020. URL `https://www.nasa.gov/sites/default/files/atoms/files/artemis_plan-20200921.pdf`.

[2] Macias, B., "Cargo Resupply Analysis For The International Space Station, Post Assembly Complete Time-Frame," *38th Aerospace Sciences Meeting & Exhibit*, 2000. https://doi.org/10.2514/6.2000-7, URL https://arc.aiaa.org/doi/10.2514/6.2000-7.

[3] Johnson, N. L., "Space traffic management concepts and practices," *Acta Astronautica*, Vol. 55, No. 3-9, 2004, pp. 803–809. https://doi.org/10.1016/j.actaastro.2004.05.055, URL https://www.sciencedirect.com/science/article/pii/S0094576504001754.

[4] Grogan, P. T., Yue, H. K., and Weck, O. d., "Space Logistics Modeling and Simulation Analysis using SpaceNet: Four Application Cases," *AIAA Space 2011 Conference & Exposition*, 2011. https://doi.org/10.2514/6.2011-7346, URL https://arc.aiaa.org/doi/pdf/10.2514/6.2011-7346.

[5] Taylor, C., Song, M., Klabjan, D., de Weck, O., and Simchi-Levi, D., "Modeling Interplanetary Logistics: A Mathematical Model for Mission Planning," *SpaceOps*, 2006. https://doi.org/10.2514/6.2006-5735, URL https://arc.aiaa.org/doi/10.2514/6.2006-5735.

[6] Ishimatsu, T., de Weck, O., and Hoffman, J., "A Generalized Multi-Commodity Network Flow Model for the Earth-Moon-Mars Logistics System," *Journal of Spacecraft and Rockets*, Vol. 53, No. 1, 2016. https://doi.org/10.2514/1.A33235, URL https://arc.aiaa.org/doi/10.2514/1.A33235.

[7] Ho, K., de Weck, O., Hoffman, J. A., and Shishko, R., "Dynamic modeling and optimization for space logistics using time-expanded networks," *Acta Astronautica*, Vol. 105, No. 2, 2014, pp. 428–443. https://doi.org/10.1016/j.actaastro.2014.10.026, URL https://www.sciencedirect.com/science/article/pii/S0094576514004044.

[8] Chen, H., and Ho, K., "Integrated Space Logistics Mission Planning and Spacecraft Design with Mixed-Integer Nonlinear Programming," *Journal of Spacecraft and Rockets*, Vol. 55, No. 2, 2017. https://doi.org/10.2514/1.A33905, URL https://arc.aiaa.org/doi/full/10.2514/1.A33905.

[9] Howell, J. T., Mankins, J. C., and Fikes, J. C., "In-Space Cryogenic Propellant Depot stepping stone," *Acta Astronautica*, Vol. 59, No. 1-5, 2006, pp. 230–235. https://doi.org/10.1016/j.actaastro.2006.02.019, URL https://ui.adsabs.harvard.edu/abs/2006AcAau..59..230H/abstract.

[10] Jagannatha, B. B., and Ho, K., "Event-Driven Network Model for Space Mission Optimization with High-Thrust and Low-Thrust Spacecraft," *Journal of Spacecraft and Rockets*, Vol. 57, No. 3, 2020. https://doi.org/10.2514/1.A34628, URL https://arc.aiaa.org/doi/10.2514/1.A34628.

[11] Ho, K., Gerhard, K., Nicholas, A. K., Buck, A. J., and Hoffman, J., "On-orbit depot architectures using contingency propellant," *Acta Astronautica*, Vol. 96, 2014, pp. 217–227. https://doi.org/10.1016/j.actaastro.2013.11.023, URL https://www.researchgate.net/publication/260016812_On-orbit_depot_architectures_using_contingency_propellant.

[12] Hoffman, J., Ishimatsu, T., Ohkami, Y., and de Weck, O., "A Proposal for Graph-Theoretic Modeling Approach to Resource-Economy in Spaceflight Campaign Logistics," *AIAA SPACE 2011 Conference & Exposition*, 2011. https://doi.org/2514/6.2011-7347, URL https://arc.aiaa.org/doi/10.2514/6.2011-7347.

[13] Myers, D. D., "Space Transportation System Overview and Program Plans," Tech. rep., National Aeronautics and Space Administration, June 1970.

[14] Mammarella, M., Vernicari, P. M., Paissoni, C. A., and Viola, N., "How the Lunar Space Tug can support the cislunar station," *Acta Astronautica*, Vol. 154, No. 1, 2019, pp. 181–194. https://doi.org/10.1016/j.actaastro.2018.04.032, URL https://www.sciencedirect.com/science/article/pii/S0094576517315175.

[15] Morales, F., Keenan, M., Simard, N., Sorrentino, R., and Vegesna, A., "Cislunar Operations Vehicle to Enable Resupply," Tech. rep., Georgia Institute of Technology Aerospace Systems Design Laboratory, May 2022.

[16] Merino, F., Risberg, J. A., and Hill, M., "Orbital Refill Of Propulsion Vehicle Tankage," Tech. rep., National Aeronautics and Space Administration, February 1980. URL https://ntrs.nasa.gov/citations/19800009811.

[17] Pino, P., Carabellese, D., Giuliani, M., Marchino, L., and Nambiar, S., "Functional and Concept Trade-off Analysis for a mission architecture for Moon and Cis-Lunar Orbit," *AIAA Propulsion and Energy Forum*, 2019. https://doi.org/10.2514/6.2019-3885, URL https://arc.aiaa.org/doi/10.2514/6.2019-3885.

[18] Zegler, F., and Kutter, B., "Evolving to a Depot-Based Space Transportation Architecture," *AIAA Space 2010 Conference & Exposition*, 2010. https://doi.org/10.2514/6.2010-8638, URL https://arc.aiaa.org/doi/10.2514/6.2010-8638.

[19] Jones, C. A., Clark, M., Pensado, A., Ivanco, M. L., Reeves, D., Judd, E., and Klovstad, J., "Cost Breakeven Analysis of Lunar ISRU for Human Lunar Surface Architectures," *70th International Astronautical Congress*, 2019. https://doi.org/IAC-19-D4.5.15, URL https://ntrs.nasa.gov/citations/20200002704.

[20] Hall, L., "In-Situ Resource Utilization (ISRU)," Tech. rep., National Aeronautics and Space Administration, April 2020. URL https://www.nasa.gov/isru.

[21] Smith, H., "Intuitive Machines Announce Landing Site Location for Lunar Drill," Tech. rep., National Aeronautics and Space Administration, November 2021. URL https://www.nasa.gov/feature/nasa-intuitive-machines-announce-landing-site-location-for-lunar-drill.

[22] "Falcon Users Guide," Tech. rep., Space Exploration Technologies Corporation, September 2021. URL https://www.spacex.com/media/falcon-users-guide-2021-09.pdf.

[23] Harbaugh, J., "Space Launch System: America's Rocket for Deep Space Exploration," Tech. rep., National Aeronautics and Space Administration, July 2022. URL https://www.nasa.gov/exploration/systems/sls/fs/sls.html.

[24] Creech, S., "NASA's Space Launch System: A Capability for Deep Space Exploration," Tech. rep., National Aeronautics and Space Administration, April 2014. URL https://www.nasa.gov/sites/default/files/files/Creech_SLS_Deep_Space.pdf.

[25] DeJean, G. B., King, J., Pannell, B., and Shiue, Y.-S. P., "Lunar Cargo Lander Design," *Huntsville Simulation Conference*, 2004.

[26] Ramos, E. M., Robertson, B., Diaz, M. J., and Mavris, D., "Development of a Lunar Lander Modeling and Simulation Capability," *AIAA Scitech 2022 Forum*, 2022. https://doi.org/10.2514/6.2022-0380, URL https://arc.aiaa.org/doi/abs/10.2514/6.2022-0380.

[27] Ramos, E. M., Robertson, B., Diaz, M. J., and Mavris, D., "A Conceptual Design Study for an Unmanned, Reusable Cargo Lunar Lander," *70th International Astronautical Congress*, 2019. URL https://ntrs.nasa.gov/citations/20190033382.

[28] "Orbital CRS-3 Mission To The International Space Station," Tech. rep., National Aeronautics and Space Administration, October 2014. URL https://www.nasa.gov/sites/default/files/files/Orbital_CRS3_press_kit.pdf.

[29] Gnegel, F., and Fügenschuh, A., "Branch-and-refine for solving time-expanded MILP formulations," *Computers & Operations Research*, Vol. 149, 2022. https://doi.org/10.1016/j.cor.2022.106043, URL https://www.sciencedirect.com/science/article/pii/S0305054822002738#b29.

[30] Skutella, M., *An Introduction to Network Flows over Time*, Springer, 2008, Chap. 21, pp. 451–482.

[31] Jones, H. W., "Estimating the Life Cycle Cost of Space Systems," *45th International Conference on Environmental Systems*, July. URL https://ntrs.nasa.gov/citations/20160001190.

[32] Street, D., and Wilhite, A., "A Scalable Orbital Propellant Depot Design," Tech. rep., Georgia Institute of Technology Space Systems Design Laboratory, April 2006. URL https://ssdl.gatech.edu/sites/default/files/ssdl-files/papers/mastersProjects/StreetD-8900.pdf.

[33] Price, H., Shishko, R., Mrozinski, J., and Woolley, R., "Concept for 2033 Crewed Mars Orbital Mission with Venus Flyby," *Journal of Spacecraft and Rockets*, 2022. https://doi.org/10.2514/1.A35437, URL https://arc.aiaa.org/doi/full/10.2514/1.A35437.

[34] Allen, B., "Human Needs: Sustaining Life During Exploration," Tech. rep., National Aeronautics and Space Administration, April 2007. URL https://www.nasa.gov/vision/earth/everydaylife/jamestown-needs-fs.html.

[35] Watters, P. B., and Schaezler, R. N., "International Space Station (ISS) Metabolic Oxygen Consumption for Expeditions 12," *36th International Conference on Environmental Systems*, 2006. https://doi.org/10.4271/2006-01-2090, URL https://doi.org/10.4271/2006-01-2090.

[36] Kauderer, A., "Higher Altitude Improves Station's Fuel Economy," Tech. rep., National Aeronautics and Space Administration, February 2011. URL https://www.nasa.gov/mission_pages/station/expeditions/expedition26/iss_altitude.html.

[37] Guzzetti, D., Zimovan, E. M., Howell, K. C., and Davis, D. C., "Stationkeeping Analysis for Spacecraft in Lunar Near Rectilinear Halo Orbits," *American Astronautical Society*, 2017. URL https://engineering.purdue.edu/people/kathleen.howell.1/Publications/Conferences/2017_AAS_GuzZimHowDav.pdf.

[38] Sullivan, B., and Akin, D., "Satellite Servicing Opportunities In Geosynchronous Orbit," *AIAA SPACE 2012 Conference & Exposition*, 2012. https://doi.org/10.2514/6.2012-5261, URL https://arc.aiaa.org/doi/10.2514/6.2012-5261.

[39] Roberts, T. G., "Popular Orbits 101," *Aerospace Security*, 2017. URL https://aerospace.csis.org/aerospace101/earth-orbit-101/.

[40] Kasaboski, D., and Bokhari, H., "Global Satellite Manufacturing and Launch Markets," *Northern Sky Research*, Vol. 12, No. 1, 2022. URL https://www.globenewswire.com/en/news-release/2022/06/21/2465718/0/en/NSR-s-Global-Satellite-Manufacturing-Launch-Report-Projects-633-Billion-Market-by-2031.html.

[41] Hadhazy, A., "The Perilous Road to Mars," *Aerospace America*, 2018. URL https://aerospaceamerica.aiaa.org/features/the-perilous-road-to-mars/.

[42] Kennedy, L. D., "NASA Lunar Lander Reference Design," Tech. Rep. NASA/TP-2019–220391, National Aeronautics and Space Administration, November 2019. URL https://ntrs.nasa.gov/citations/20190033128.

[43] Holt, J. B., and Monk, T. S., "Propellant Mass Fraction Calculation Methodology for Launch Vehicles and Application to Ares Vehicles," *AIAA SPACE 2009 Conference & Exposition*, 2009. https://doi.org/10.2514/6.2009-6655, URL https://arc.aiaa.org/doi/10.2514/6.2009-6655.